PERGAMON

Journal of Structural Geology 21 (1999) 1693–1713

JOURNAL OF STRUCTURAL GEOLOGY

www.elsevier.nl/locate/jstrugeo

Ultracataclasis, sintering, and frictional melting in pseudotachylytes from East Greenland

Daniel Curewitz*, Jeffrey A. Karson

Division of Earth and Ocean Sciences, Duke University, Durham, NC 27708-0229, USA

Received 9 July 1998; accepted 8 June 1999

Abstract

Large volumes of pseudotachylyte (an intrusive, fault-related rock interpreted to form by a combination of cataclasis and melting) occur in Tertiary normal faults and accommodation zones along ~400 km of the East Greenland volcanic rifted margin. Analysis of representative pseudotachylyte samples reveals a wide range of mesoscopic and microscopic textures, mineralogies, and chemistries in the aphanitic pseudotachylyte matrix. Three distinct types of pseudotachylyte (referred to as angular, rounded and glassy) are identified based on these characteristics. Angular pseudotachylyte (found primarily in dike-like reservoir zones) is characterized by angular grains visible on all scales, with micron-scale fragments of mica and amphibole. Its matrix is enriched in Fe_2O_3, MgO, and TiO_2 relative to the host rock, with minor increases in CaO, K_2O, and small decreases in Na_2O. Rounded pseudotachylyte is found in reservoir zones, injection veins (pseudotachylyte-filled extension fractures), and fault veins (small faults with pseudotachylyte along their surfaces). It is characterized by smooth-surfaced, compacted grains on microscopic scales, and encloses rounded, interpenetrative lithic clasts on outcrop scale. Its matrix is enriched in Fe_2O_3, MgO, TiO_2, and Al_2O_3 relative to the host rock, with minor depletion in Na_2O and K_2O. Glassy pseudotachylyte is found primarily along fault surfaces. Its matrix is characterized by isotropic, conchoidally fractured material containing microscopic, strain-free amphibole phenocrysts, and is enriched in TiO_2, Al_2O_3, K_2O, Fe_2O_3, MgO, CaO, and Na_2O relative to the host rock. These observations suggest that angular pseudotachylyte was produced by cataclasis, with enrichment in metallic oxides resulting from preferential crushing of mechanically weak amphibole and mica minerals found in the gneissic host rock. Cataclasis and concomitant frictional heating resulted in the textural and chemical modification of angular pseudotachylyte by sintering or melting, producing rounded and glassy pseudotachylyte, respectively. Compositional and textural observations constrain the temperatures reached during frictional heating (700–900°C) which in turn delimit the amount of frictional heat imparted to the pseudotachylytes during slip. Our results suggest that the East Greenland pseudotachylytes formed during small seismic events along faults at shallow crustal levels. Consistent relative ages and widespread occurrence of pseudotachylyte-bearing faults in East Greenland suggest that widespread microseismicity accompanied the early development of this volcanic rifted margin.

1. Introduction

Pseudotachylytes are fault rocks consisting of varying proportions of rounded to angular clasts of country rock surrounded by dark-colored, aphanitic matrix and generally intruding the surrounding host rocks. Pseudotachylyte occurs along thrust, strike-slip, and normal faults (McKenzie and Brune, 1972; Sibson, 1975; Magloughlin and Spray, 1992; Swanson, 1992; Spray, 1995), along major unconfined 'superfaults' (Spray, 1997), in meteorite impact structures (Lambert, 1981; Dressler, 1984; Reimold, 1991; Magloughlin and Spray, 1992; Reimold and Colliston, 1994; Spray and Thompson, 1995; Spray, 1997), and along the base of major landslides (Scott and Drever, 1953; Erismann, 1979; Masch et al., 1985). Frictional melts have been produced in experiments, during industrial drilling, and in quarrying operations (Spray, 1987, 1989, 1992, 1995; Kennedy and Spray, 1992). The diversity of pseudotachylyte textures and settings

* Corresponding author.
E-mail address: curewitz@eos.duke.edu (D. Curewitz)

0191-8141/99/$ - see front matter
PII: S0191-8141(99)00119-4

has fostered disagreement over their origin and formation mechanism(s) (e.g. Sibson, 1975; Wenk, 1978; Shimamoto and Nagahama, 1992; Spray, 1995). Recent field, laboratory and experimental investigations have shown that 'pseudotachylyte' can be viewed as an umbrella term, covering a range of textures from ultracataclasite to melt formed by a combination of comminution and frictional heating during faulting at seismic slip rates ($>10^{-1}$ m s^{-1}) (Magloughlin and Spray, 1992; Spray, 1995).

This paper concerns an investigation of pseudotachylyte found in Early Tertiary normal faults and accommodation zones along ~400 km of the East Greenland coast. An endogenic tectonic origin for these pseudotachylytes (rather than association with impact structures, e.g. Lambert, 1981; Thompson and Spray, 1994; Spray, 1997) is clearly indicated by their occurrence within Tertiary-age rift-related fault zones. Pseudotachylytes occur in a variety of mesoscopic settings within these fault zones—in >10-m-wide dike-like bodies ('reservoir zones'), in extension fractures ('injection veins'), and along fault surfaces ('fault veins'). Microscopic and chemical analyses of pseudotachylytes and host rocks from these structural settings reveal three textures: (1) angular ultracataclasite found mainly in reservoir zones; (2) rounded pseudotachylyte found in reservoir zones, injection veins, and fault veins; and (3) glassy pseudotachylyte found mainly in fault veins. All of these are enriched in metallic oxides relative to their host rocks. These relationships suggest a textural evolution of pseudotachylyte as a result of seismic slip and frictional heating. Initially, ultracataclasite that is preferentially enriched in relatively weak mafic minerals (amphibole and mica) forms by asperity grinding and comminution. Preferential inclusion of mafic minerals in this ultracataclasite controls the metal oxide enrichment found in the other textural types, and noted in many pseudotachylyte studies (e.g. Magloughlin and Spray, 1992). The ultracataclasite is subsequently modified to varying degrees by frictional heating, either by sintering (densification of granular material by solution transfer processes at elevated temperatures, e.g. Luan and Patterson, 1992) or melting. Interpretation of the structural settings, textures, and chemistries of these pseudotachylytes suggests that they formed during relatively low-magnitude earthquakes that may have accompanied Early Tertiary continental rifting in East Greenland.

2. Geologic setting

East Greenland was separated from Scandinavia and Western Europe in the Early Tertiary, forming the rifted margins that now bound the northeast Atlantic (Brooks and Nielsen, 1982; Larsen, 1990; Eldholm and Grue, 1994). Fieldwork for this study was conducted along the coast of East Greenland south of Kangerlussuaq Fjord (Fig. 1). The study area has undergone ~6 km of uplift in the Tertiary (Gleadow and Brooks, 1979; Brooks and Nielsen, 1982; Hansen, 1996). Uplift and erosion have exposed basement composed of Archean–Proterozoic granitic gneiss with up to 100-m-wide amphibolite bands (Bridgewater et al., 1976). Local Cretaceous–Tertiary sedimentary deposits, a coast-parallel dike swarm, extensive (>5 km thick) flood basalts, and several mafic and silicic intrusions characterize the general geology of the East Greenland volcanic rifted margin in this area (Nielsen, 1975, 1978; Brooks and Nielsen, 1982; Pedersen et al., 1997; Karson et al., 1998; Karson and Brooks, 1999).

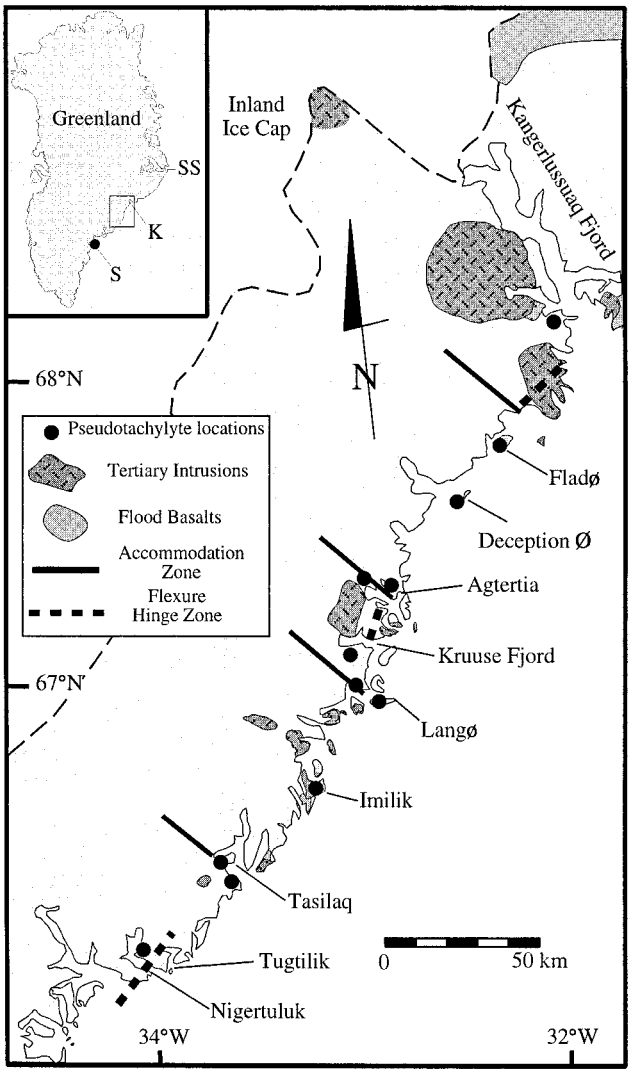

Fig. 1. Geological map of study areas in East Greenland. (a) Location map of Greenland: S = Skjoldungen, K = Kangerlussuaq Fjord, SS = Scoresby Sund. (b) Highly generalized map of the study areas south of Kangerlussuaq Fjord, sample sites marked by filled circles.

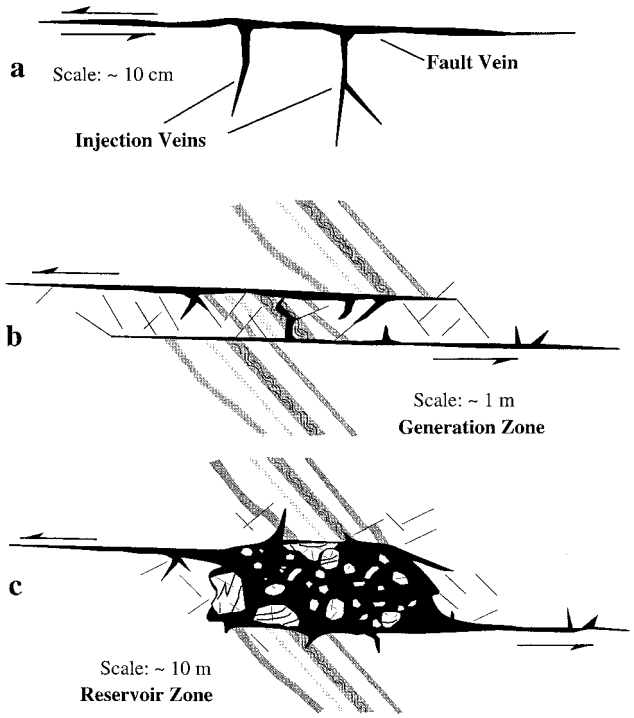

Fig. 2. Schematic diagram showing the geometry of pseudotachylyte-bearing faults. (a) Fault veins and injection veins. (b) Generation zones. (c) Pseudotachylyte breccia bodies. See text for descriptions.

The flood basalts thicken towards the coast and have steeper eastward dips (i.e. towards the center of the ancient rift). The older dikes in the coastal dike swarm dip gently landward (20–40° west), and younger dikes are near vertical (Wager and Deer, 1938; Nielsen, 1978; Myers, 1980). Together these features define a coast-parallel flexure formed by normal and strike- to oblique-slip faulting, distributed cataclasis, and minor bedding-parallel slip in sediments and lavas (Nielsen, 1975; Brooks and Nielsen, 1982; Karson et al., 1998; Karson and Brooks, 1999).

Pseudotachylytes are found in the Tertiary fault zones that accommodated the formation of the flexure. Coast-perpendicular strike-slip and oblique-slip faults link normal faults and accommodate along-strike variations in mechanical extension, magmatic dilation, and flexural kinematics (Karson and Brooks, 1999). Pseudotachylyte is especially common in these accommodation zones (Fig. 1). ^{40}Ar–^{39}Ar dating of cross-cutting igneous intrusions (Tegner et al., 1998) and one pseudotachylyte sample (Karson et al., 1998) indicates an Early Tertiary age for these fault zones. The relationships between structures and intrusions indicate broadly coeval faulting (and pseudotachylyte formation) and magmatism during formation of the flexure (Nielsen, 1975, 1978; Karson et al., 1998; Karson and Brooks, 1999).

Relatively late, landward-dipping normal faults cut the flexure and related faults, the coast-parallel dike swarm, and the seaward dipping sedimentary and volcanic units. These faults have been documented in ODP drill cores, offshore seismic surveys, and onshore in East Greenland, and are probably associated with subsidence of the newly formed rifted margin (Nielsen and Brooks, 1981; Clift et al., 1995; Pedersen et al., 1997; Larsen and Saunders, 1998; Karson and Brooks, 1999). Inspection of thin sections from ODP Hole 917 reveals that rocks from these younger faults, originally reported as pseudotachylyte (Larsen et al., 1994), are actually hydrothermally altered fault breccias.

3. Pseudotachylyte vein geometry and characteristics

Outcrop relationships between pseudotachylyte and surrounding rocks (Fig. 2) have been described in detail by many workers (Sibson, 1975; Grocott, 1981; Swanson, 1992). Fault veins are thin layers of pseudotachylyte (<2 cm wide) along faults with measurable displacements. Injection veins are narrow ($\sim$2 cm wide), elongate ($\sim$1 m long) extension fractures filled with pseudotachylyte. Generation zones occur in fault zones where pseudotachylyte is thought to have formed during seismic slip (Grocott, 1981) and are composed of linked faults and extension fractures with associated arrays of fault and injection veins. Recently, generation zones have been recognized as overlapping tips of faults in en échelon arrays (Swanson, 1992). Reservoir zones (Sibson, 1975) are large, dike-like pseudotachylyte bodies that are commonly >10 m wide and occupy extensional voids in fault zones. The following sections describe the macro- and microscopic characteristics of the Tertiary East Greenland pseudotachylytes in these structural settings.

3.1. Characteristics of pseudotachylyte-bearing faults

The Tertiary pseudotachylyte in East Greenland is dark gray to brown or black and consists of massive, aphanitic material that exhibits conchoidal to roughly planar fractures. Fresh pseudotachylyte surfaces commonly exhibit vitreous to waxy luster. In thin section the pseudotachylyte matrix ranges from isotropic in a few cases, to 'blotchy' or variolitic in many instances. Rounded to angular clasts of host rock that vary from >1.0 m to <0.001 m in diameter are visible in the pseudotachylyte matrix, and mineral fragments as small as 10 μm across are visible in scanning electron microscope (SEM) images. Mineral veins consisting of epidote, calcite, quartz, muscovite and, in rare instances, prehnite, hematite, or limonite are visible both in hand sample and in thin section. These cross-cut the pseudotachylyte, showing that hydrothermal activity and veining post-dated pseudotachylyte generation.

Fault veins (Figs. 2a and 3a) are found in many of the fault zones investigated in East Greenland. Pseudotachylytes in fault veins are generally vitreous or waxy and exhibit conchoidal fractures in hand sample. Individual fault veins range from <1 cm wide up to 2–3 cm wide. Both 'ductile-margin' and 'sharp margin' (Thompson and Spray, 1994) fault veins are documented. In several cases, linked sets of multiple, sub-parallel, small-offset (<2 cm) fault veins are found cutting the host gneiss. The fault veins in these areas are commonly linked by injection veins and subsidiary fractures (Figs. 2b and 3b).

Injection veins (Figs. 2a and 3c) are generally <2 cm wide, and reach up to 1 m in length. Most injection veins described here have sharply defined margins with little or no displacement across the vein. Some examples exhibit textures with aligned clasts, streaks, and bands suggestive of flow. These veins are generally linked to small faults and fault veins, and it appears that material was forced from the fault veins into the injection veins. Lithic clasts are relatively abundant in injection veins, and clast margins are generally very smooth and well rounded.

Reservoir zones are commonly several meters to tens of meters wide (Figs. 2c and 3d), and in several cases their boundaries are not exposed, indicating even larger dimensions. They are made up of black to dark brown pseudotachylyte matrix and considerable quantities of variably sized, angular to rounded clasts. There is some resemblance between these dike-like bodies and breccia dikes (Lambert, 1981; Reimold and Colliston, 1994), or pseudotachylyte-bearing superfault outcrops (Spray, 1997)—features associated with meteorite impact structures. The East Greenland pseudotachylyte reservoir zones are associated with rift-related faults that developed over a substantial period of time during formation of the regional flexure and intrusion of the dike swarm. There is no evidence for ring-faults, or for shock deformation features such as multiple planar deformation features in quartz, high-pressure mineral phases (coesite or stishovite), or shatter cones, suggesting that these features are tectonic rather than impact related.

3.2. Lithic clasts

Lithic clasts are fragments of host rock surrounded by aphanitic pseudotachylyte matrix (after Magloughlin and Spray, 1992). In East Greenland they range in size from >1 m across to <0.001 m across

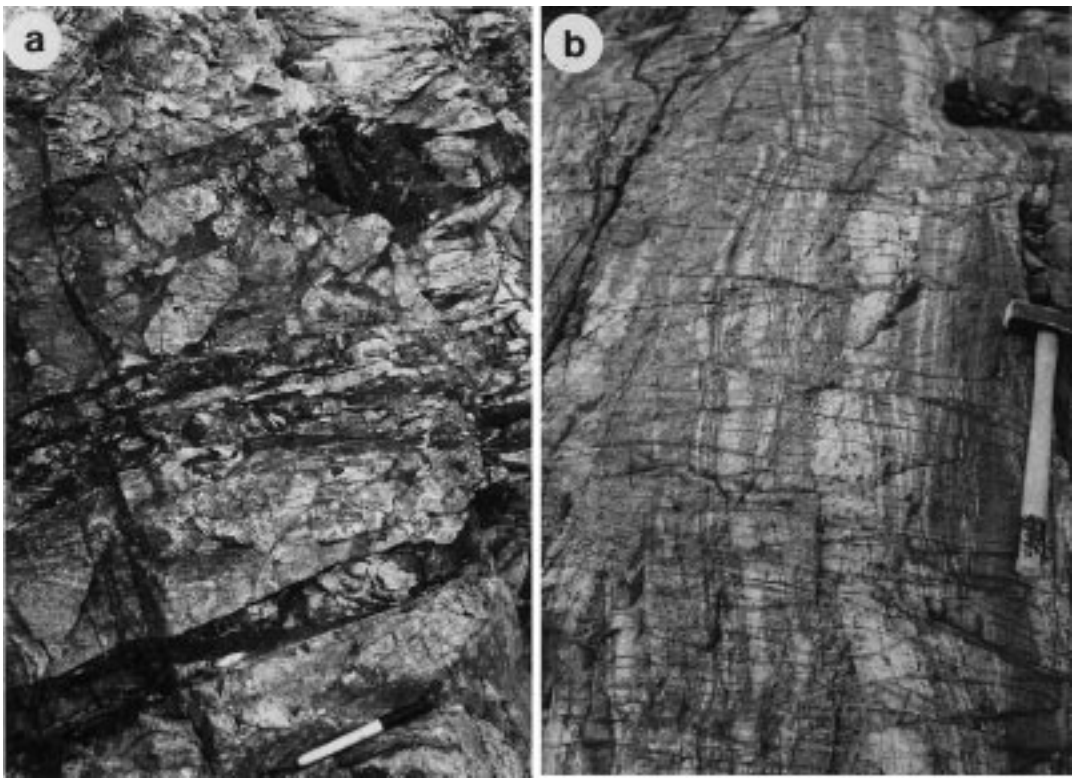

Fig. 3. Structural settings of pseudotachylyte. (a) Several parallel fault veins in basement gneiss. Dark pseudotachylyte veins have sharp contacts and enclose rounded clasts of light-colored host rock; Tasilaq. (b) Generation zone with ~2-cm-wide, linked fault veins, subsidiary fractures, and injection veins; Kruuse Fjord. (c) Irregular, ~2-cm-wide injection vein rooted in a fault zone and cutting several Reidel shears; Agtertia. (d) Reservoir zone with black, aphanitic pseudotachylyte matrix enclosing clasts up to ~1 m across; Agtertia. (e) Rounded, allocthonous clasts of mafic dike rock (dark) and gneiss (light) coexist in a reservoir zone; Langø.

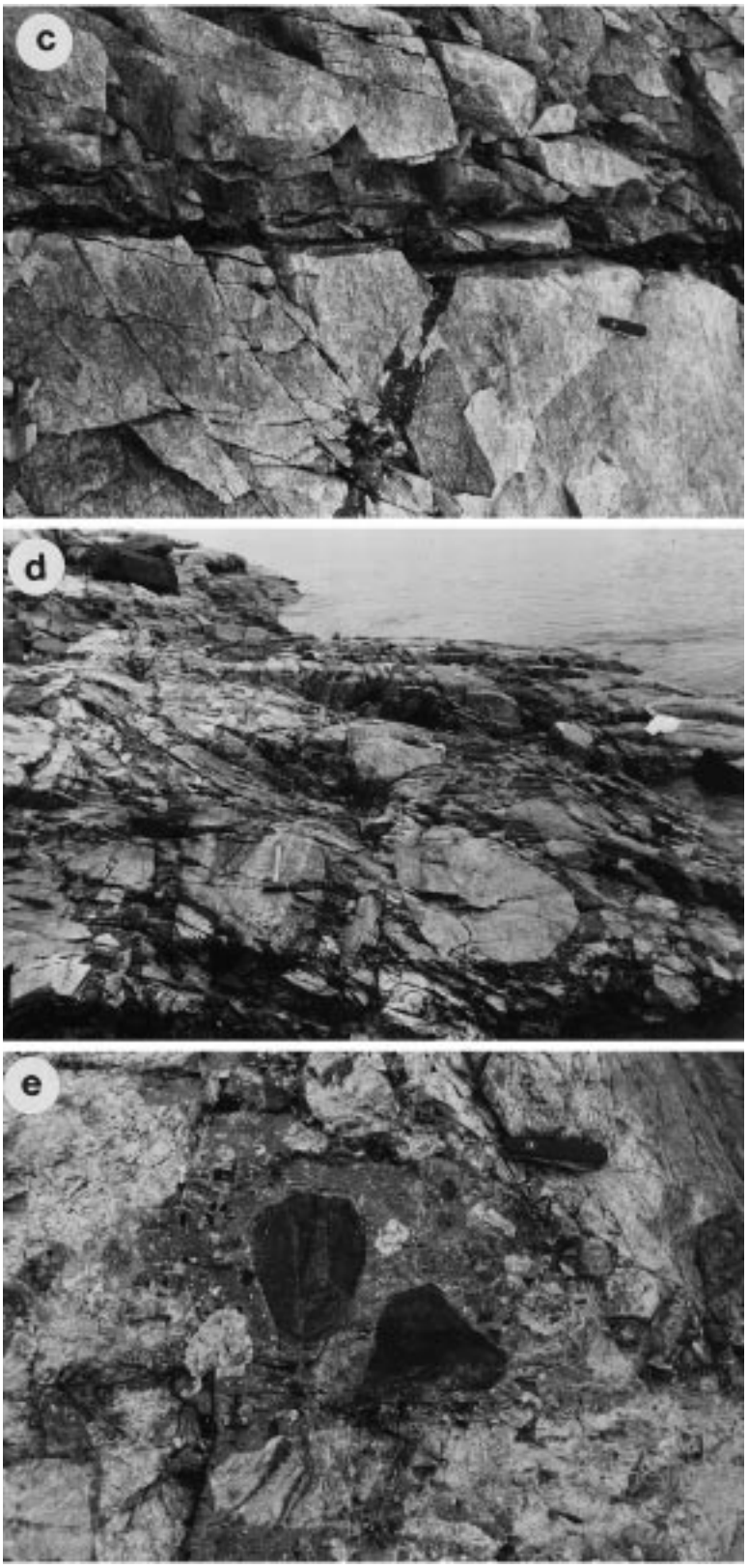

Fig. 3. (*continued*).

Table 1
Sample location, sample number, structural setting, pseudotachylyte texture, and chemical composition for each pseudotachylyte/host rock pair analysed. All values are normalized to 100% totals assuming all deviations are accounted for by loss on ignition. 'FV' refers to fault veins, 'IV' to injection veins, and RZ to reservoir zones. 'H' refers to host rock, 'P' to pseudotachylyte. 'A' to angular pseudotachylyte, 'R' to rounded pseudotachylyte, and 'G' to glassy pseudotachylyte

Location	Nigertuluk						Tasilaq						
Sample #	417420		417427		417443		417117		417473		417477		
Setting	FV		FV/IV		RZ		IV		FV/IV		FV		
H/P	H	P	H	P	H	P	H	P	H	P	H(A)	H(G)	P
Texture		G		R/G		A/R		R		R/G			G
SiO_2	91.14	72.90	68.63	57.40	71.57	61.14	50.50	56.20	64.98	42.78	51.51	70.18	50.34
TiO_2	0.06	0.32	0.26	0.73	0.20	1.01	0.59	2.40	0.23	0.15	0.93	0.17	0.84
$A1_2O_3$	4.45	14.36	17.32	17.68	13.06	16.02	4.00	13.09	14.21	2.59	15.49	16.71	17.40
Fe_2O_3	0.84	1.90	2.59	7.58	2.06	7.06	12.14	14.04	4.20	45.82	10.10	2.27	11.31
MnO	0.01	0.02	0.03	0.09	0.02	0.05	0.21	0.18	0.06	0.04	0.16	0.03	0.13
MgO	0.22	0.78	1.18	2.08	0.58	2.06	15.31	2.90	4.51	2.45	8.74	1.16	5.60
CaO	1.00	2.44	2.58	6.97	6.05	3.96	16.67	6.53	5.64	6.06	9.43	3.96	9.08
Na_2O	1.88	6.07	5.97	4.51	4.72	3.65	0.32	3.18	4.13	0.00	2.87	4.71	5.02
K_2O	0.40	1.19	1.44	2.96	1.73	5.04	0.26	1.48	2.04	0.11	0.77	0.81	0.29
Sr	103.46	311.81	746.28	822.07	379.78	215.89	41.56	555.44	254.13	269.76	1040.60	1013.45	1253.72
Ba	131.65	478.29	716.57	1369.46	567.24	2432.50	176.54	1019.76	740.70	55.12	408.28	421.75	254.99
SUM	100.00	100.00	100.00	100.00	100.00	100.00	100.00	100.00	100.00	100.00	100.00	100.00	100.00
LOI	0.52	0.93	1.23	1.12	4.33	3.63	0.82	1.83	5.01	5.18	2.68	0.95	6.56

Location	Flad Ø		Agtertia						Lang Ø			
Sample #	428436		428449		428453		428471		428472		428473	
Setting	FV		IV		RZ		RZ		FV		RZ	
H/P	H	P	H	P	H	P	H	P	H	P	H	P
Texture		G		R		A/R		A/R		G		R
SiO_2	51.40	44.30	70.86	63.81	73.31	66.34	75.22	64.25	47.39	47.80	73.48	69.01
TiO_2	0.19	0.41	0.45	0.92	0.48	1.20	0.08	0.65	0.09	0.26	0.29	0.41
$A1_2O_3$	7.72	11.48	15.28	16.80	14.06	13.61	13.80	14.39	1.30	4.83	14.30	15.18
Fe_2O_3	12.16	15.78	3.24	6.01	1.59	7.32	0.96	7.14	10.65	10.10	2.23	3.92
MnO	0.26	0.30	0.03	0.07	0.04	0.11	0.01	0.06	0.13	0.07	0.02	0.04
MgO	12.38	16.89	0.82	1.79	0.28	1.23	0.44	3.52	35.16	31.70	0.64	1.34
CaO	14.46	9.99	3.49	4.64	1.10	2.89	2.00	3.63	5.32	4.73	1.69	1.99
Na_2O	1.19	0.65	4.70	4.10	3.06	3.03	3.35	2.66	-0.06	0.06	3.58	3.26
K_2O	0.23	0.20	1.11	1.86	6.07	4.28	4.12	3.70	0.02	0.45	3.76	4.86
Sr	267.97	91.21	646.20	893.92	211.78	205.46	191.68	137.50	13.04	17.37	271.09	253.49
Ba	42.74	66.14	638.61	1006.01	1576.18	1212.99	2557.94	1618.81	4.69	100.25	1288.47	1594.75
SUM	100.00	100.00	100.00	100.00	100.00	100.00	100.00	100.00	100.00	100.00	100.00	100.00
LOI	1.55	5.62	0.36	0.43	0.25	0.27	0.44	0.37	2.53	4.07	0.80	0.45

Location	Lang Ø				Deception Ø		Skjoldungen		Kruuse F.				
Sample #	428474		428494		438523		91-234		428495		428499		
Setting	IV		RZ		FV		IV		FV		RZ		
H/P	H	P	H	P	H	P	H	P	H	P	H	P1	P2
Texture		R		R		A/G		R/G		G		R	R
SiO_2	69.72	67.55	69.74	67.19	74.60	64.81	67.71	65.35	62.99	62.10	71.63	66.60	52.96
TiO_2	0.38	0.54	0.31	0.48	0.16	0.28	0.28	0.49	0.29	0.31	0.32	0.20	1.38
$A1_2O_3$	15.48	15.85	16.18	14.84	13.77	16.63	16.67	15.29	20.48	19.08	13.03	13.71	14.47
Fe_2O_3	3.88	4.06	1.88	5.10	1.99	4.69	3.68	5.28	3.11	5.25	4.12	5.98	11.66
MnO	0.05	0.05	0.04	0.07	0.02	0.06	0.04	0.06	0.05	0.06	0.04	0.05	0.10
MgO	1.26	1.19	0.70	2.38	0.41	1.39	1.52	2.94	0.90	1.73	1.96	2.92	6.29
CaO	3.37	2.94	2.71	3.62	2.10	4.32	3.97	4.49	4.44	4.11	5.68	7.38	9.44

Table 1 (*continued*)

Location	Lang Ø				Deception Ø		Skjoldungen		Kruuse F.				
Sample #	428474		428494		438523		91-234		428495		428499		
Setting	IV		RZ		FV		IV		FV		RZ		
H/P	H	P	H	P	H	P	H	P	H	P	H	P1	P2
Texture		R		R		A/G		R/G		G		R	R
Na_2O	4.65	3.61	3.78	3.74	3.70	7.71	4.66	4.17	6.36	5.40	2.21	1.59	0.94
K_2O	1.21	4.22	4.66	2.58	3.25	0.12	1.47	1.91	1.38	1.95	1.02	1.57	2.75
Sr	317.27	270.63	411.52	329.28	165.55	228.31	500.22	615.46	411.25	543.43	100.06	117.48	84.43
Ba	200.11	1422.12	1457.96	1364.91	1028.70	27.91	623.17	836.19	687.63	911.35	247.11	205.49	315.37
SUM	100.00	100.00	100.00	100.00	100.00	100.00	100.00	100.00	100.00	100.00	100.00	100.00	100.00
LOI	0.82	0.53	0.52	0.66	0.36	0.36	1.45	1.65	0.96	0.89	1.02	0.86	0.91

(Fig. 3d and e), and are angular to rounded in profile. The gneissic foliation in the clasts is commonly found at varying angles to the surrounding foliation, indicating significant rotation. Polymict pseudotachylytes contain both local and allocthonous clasts (Fig. 3e), indicating significant amounts of transport (at least several meters) along the fault zones. The clasts are highly fractured and invaded by pseudotachylyte veins. Cross-cutting relationships show that many intra-clast fractures and veins are truncated by texturally distinct pseudotachylyte at the clast edges. These cross-cutting relationships could be interpreted as evidence for multiple pseudotachylyte generations, or as evidence for rapid formation of large reservoir zones from generation zones (e.g. Sibson, 1975).

Where lithic clasts are well rounded, they commonly indent one another in a manner similar to that found in meta-conglomerates affected by pressure solution (Mosher, 1976). Rounded clasts in thin section commonly exhibit haloes of progressively smaller quartz and feldspar neoblasts toward their margins. These textures suggest that rounding occurred by chemical reaction and diffusion along clast margins, or annealing by contact with the hot pseudotachylyte matrix (Magloughlin and Spray, 1992; Magloughlin, 1998). These interpretations will be addressed in more detail in the following sections.

4. Analytical methods

Eighteen samples were selected from nine locations along the East Greenland margin, representing the full range of structural settings and vein geometries in this region (Table 1). Textural, chemical, and mineralogical analyses were conducted on each sample using a variety of analytical techniques. Comparison of these data among pseudotachylytes found in fault veins, injection veins, and reservoir zones sheds light on pseudotachylyte generation and preservation in these different areas.

Polished thin sections from the selected samples were described, photographed, and then carbon-coated to ~250 Å thickness in a Denton Vacuum DV-502A vacuum evaporator in preparation for microprobe analysis. Microprobe analyses were made using a Cameca Camebax microprobe set to 15 keV, 20 nA. All analyses were made using the quantitative energy dispersive spectrometer via the FLAME® operating system with natural mineral standards. Point, wide-beam (20–50 μm), and raster analyses were made at various scales and in different domains of each thin section in order to determine the composition of pseudotachylyte matrices, clasts, and other features, such as haloes around grains, opaque mineral compositions, and hydrothermal vein compositions.

Chips of pseudotachylyte and host rocks were taken from the hand samples, cleaned, and crushed in a ring mill. Loss on ignition was measured by heating the powdered samples for 1 h at 900°C. The samples were then weighed, mixed with lithium metaborate flux, melted, and dissolved in nitric acid solution. The major element chemistry of the pseudotachylyte and host rock samples was then determined using a Directly Coupled Plasma (DCP) spectrometer.

Samples were imaged using a Phillips 501 scanning electron microscope (SEM). Representative pieces of veins, clasts, and host rock were mounted on SEM stubs; the stub and sample base were coated with electro-conductive carbon paint, and the entire sample gold coated in an ISI sputter coater. Coated samples were then imaged at a variety of magnifications in order to highlight textural characteristics. Additional images were taken using the microprobe, and these images include semi-quantitative element maps of selected areas of the thin sections.

The comparative mineralogy of pseudotachylyte veins and host rocks was determined semi-quantitat-

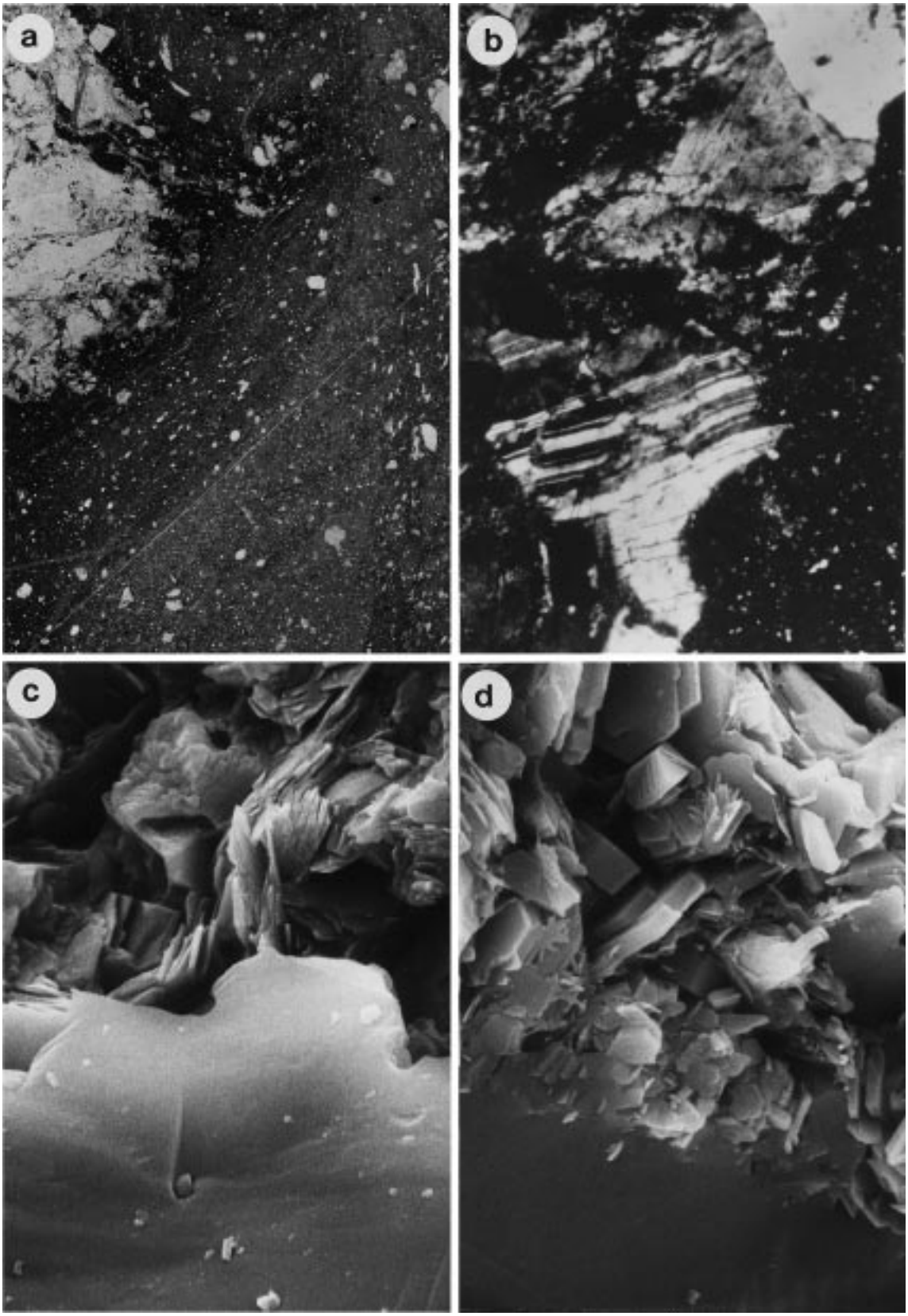

Fig. 4. Microstructures of angular pseudotachylyte. (a) Cataclastic gneiss fragments in pseudotachylyte matrix; note gradational changes near vein margin, whorls, and aligned clasts suggesting flow. Sample 428455, 20 mm across, polarized light (XPL). (b) Fragmental pseudotachylyte matrix surrounding a clast of twinned plagioclase and recrystallized quartz. Sample 428494, 2 mm across, XPL. (c) SEM image of angular fragments of mica and feldspar with obvious cleavage surfaces; grains touch at edges and points. Smooth area at the bottom of the image is a mica grain. Sample 428469, 10 μm across. (d) SEM image of typical cataclastic fault rock; Turkana, Kenya, 10 μm across.

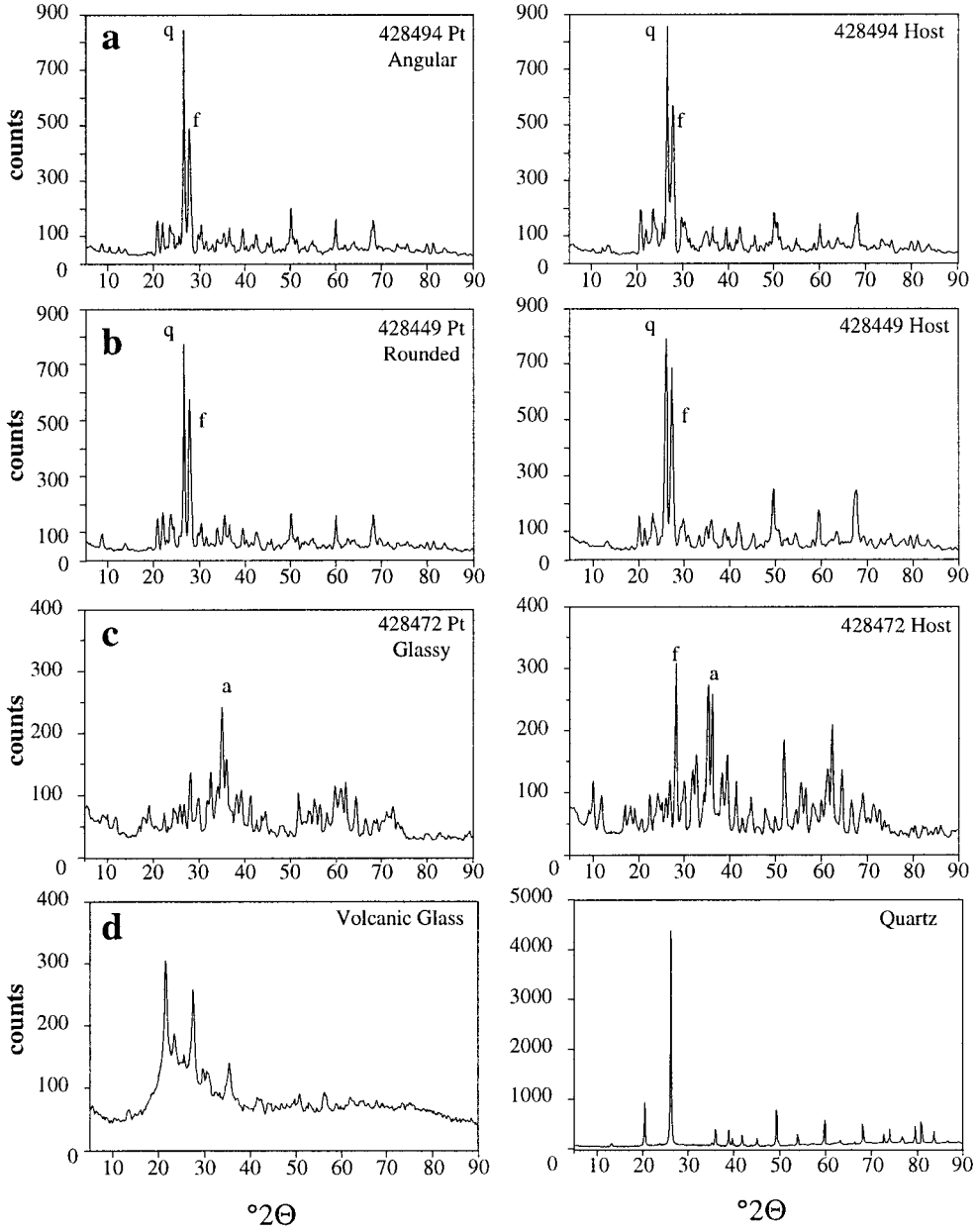

Fig. 5. Representative X-ray diffraction spectra for the three types of pseudotachylyte, with volcanic glass and quartz for reference. Mineral peaks: Pt = pseudotachylyte matrix, q = quartz, f = feldspar, a = amphibole. (a) Angular pseudotachylyte: XRD spectra of the pseudotachylyte (left) and the host rock (right). (b) Rounded pseudotachylyte. (c) Glassy pseudotachylyte. (d) Volcanic glass and quartz powder.

ively using a Phillips XRG-3000 X-Ray Diffractometer (XRD) set to 35 keV at 20 nA using a Cu-Kα_1 source. Samples were ground and sieved to ensure uniform 100 μm grain size. Weathered materials and vein materials were picked out by hand, the powder was mixed with alcohol, and this slurry was mounted on standard petrographic slides. The slides were run from 5° to 90° 2θ in steps of 0.05° 2θ, and analysed for 1.0 s per step. The resulting spectrum was analysed for peak height and position for qualitative mineralogical information, and compared to a glass standard to check for the presence of amorphous phases.

5. Results and interpretation

Three textural types of pseudotachylyte are recognized in the East Greenland sample suite: angular pseudotachylyte is essentially ultracataclasite with angular clasts and fragments on all scales; rounded pseudotachylyte contains densely packed and interlocking smooth, rounded, or polyhedral grains; and glassy pseudotachylyte has essentially igneous textures. These designations refer to the textural characteristics of the aphanitic matrix of the pseudotachylyte samples, visible only under high magnification using

optical microscope, SEM, or microprobe. The different types occur in several associations: as discrete bands of a single type, as adjacent bands of different types with sharp contacts, or as gradational mixtures. In the last two cases, the most common associations observed are angular and rounded pseudotachylyte, or rounded and glassy pseudotachylyte; only in one instance is a mixture of angular and glassy pseudotachylyte observed. Below, the chemical, mineralogical, and micron-scale characteristics of the East Greenland pseudotachylyte suite are presented within the framework of the identified textural types.

5.1. Angular pseudotachylyte

Angular pseudotachylyte is found mainly in reservoir zones and injection veins. In only one case is there angular pseudotachylyte in a fault vein. Angular pseudotachylyte exhibits no evidence for any glassy or isotropic material on any scale. Locally there are flow textures and bands defined by color changes (Fig. 4a), and by preferred orientation of elongate grains. The matrix is granular in thin section, and clasts show transgranular fractures and deformation twins indicative of cataclasis (Fig. 4b). SEM images reveal small (< 10 μm) angular grains with rough surfaces, microfractures, and partings along cleavage planes. These grains form a highly porous framework supported by point contacts (Fig. 4c). SEM images of angular pseudotachylytes exhibit characteristics similar to cataclasites from other fault zones (Fig. 4d). Lithic clasts are commonly jagged, they exhibit no haloes or recrystallization textures along clast margins, and they generally touch at point contacts with little or no indentation or interpenetration of clast margins.

X-ray diffraction (XRD) analysis of angular pseudotachylyte reveals that peak-to-background ratios are high and mineral peaks are sharp and narrow (Fig. 5a), indicating that there has been little or no change in the crystallinity of the starting material, only grain-size reduction by cataclasis.

DCP chemical analyses show that angular pseudotachylyte is depleted in SiO_2 and enriched in metallic oxides relative to the host rock. Relatively small weight-percentage decreases in SiO_2 balance the large weight-percentage increases in metallic oxides. The pseudotachylyte matrix has increased concentrations of several weight percent in Fe_2O_3, TiO_2, and MgO; relatively little change in CaO, K_2O and Ba, and small decreases in Na_2O and Sr (Fig. 6a). Silica variation diagrams (Fig. 6b) show the change in oxide abundances for individual samples. Pseudotachylyte (open symbols) and

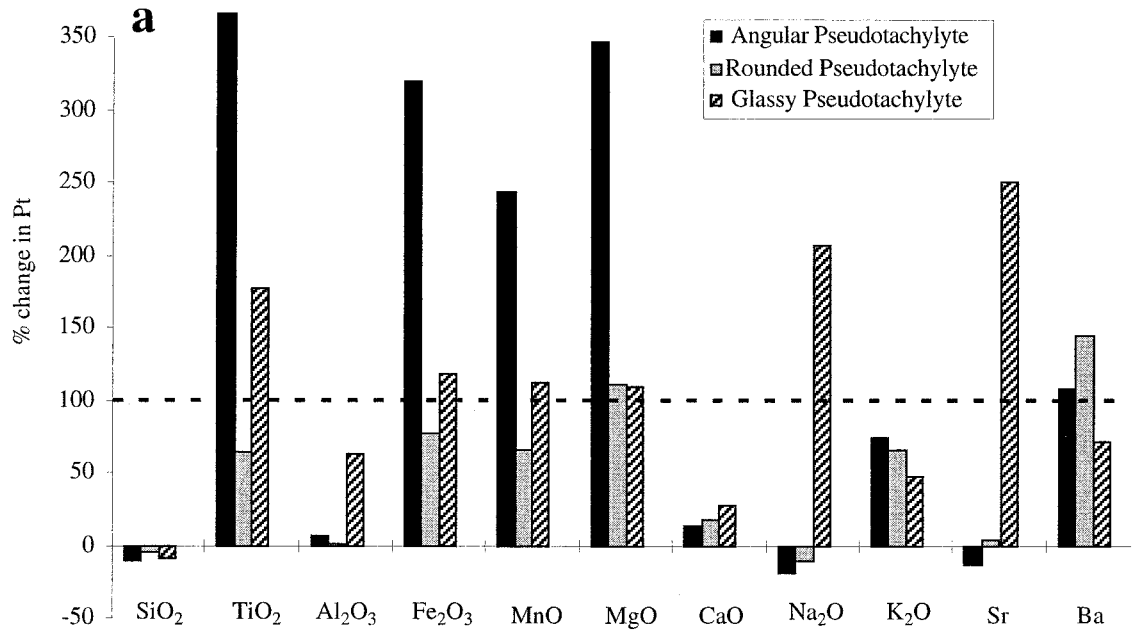

Fig. 6. Chemistry of the three pseudotachylyte types compared to their respective host rocks. (a) Bar graph depicting the normalized percent change in concentrations of major elements among angular, rounded, and glassy pseudotachylyte. Normalized percent changes in the pseudotachylyte, (abbreviated "Pt" on the y-axis of Fig. 6 (a and c) are calculated by [(pt−host)/host]*100 (Pt = oxide concentration in the pseudotachylyte, host = oxide concentration in the host rock), with each pseudotachylyte sample compared to its own host. Dashed line at 100% for reference, note that 100% change in pseudotachylyte would actually be a doubling of the weight percentage of that oxide in the pseudotachylyte relative to the host rock. (b) Silica variation diagrams showing changes in major element concentration in pseudotachylytes (open symbols) compared to their host rocks (filled symbols). Pseudotachylyte/host-rock pairs are joined by tie-lines. (c) Bar graph showing normalized percent change in loss on ignition (LOI) among the different pseudotachylyte types compared to their host rocks (same calculation as above).

their corresponding host rocks (solid symbols) are connected by tie lines. These results show consistent, steep enrichment in Fe_2O_3 and MgO in the pseudotachylyte as compared to the host rock. Enrichment in CaO and Al_2O_3 is less drastic and less consistent between samples. There is a slight, somewhat inconsistent decrease in Na_2O and K_2O. Angular pseudotachylyte has relatively lower values for loss on ignition (Fig. 6c) compared to the host rock, suggesting that volatile material has been lost from the pseudotachylyte. Wide-area (> 100 μm) raster microprobe analyses of angular pseudotachylyte show the same enrichment in metallic

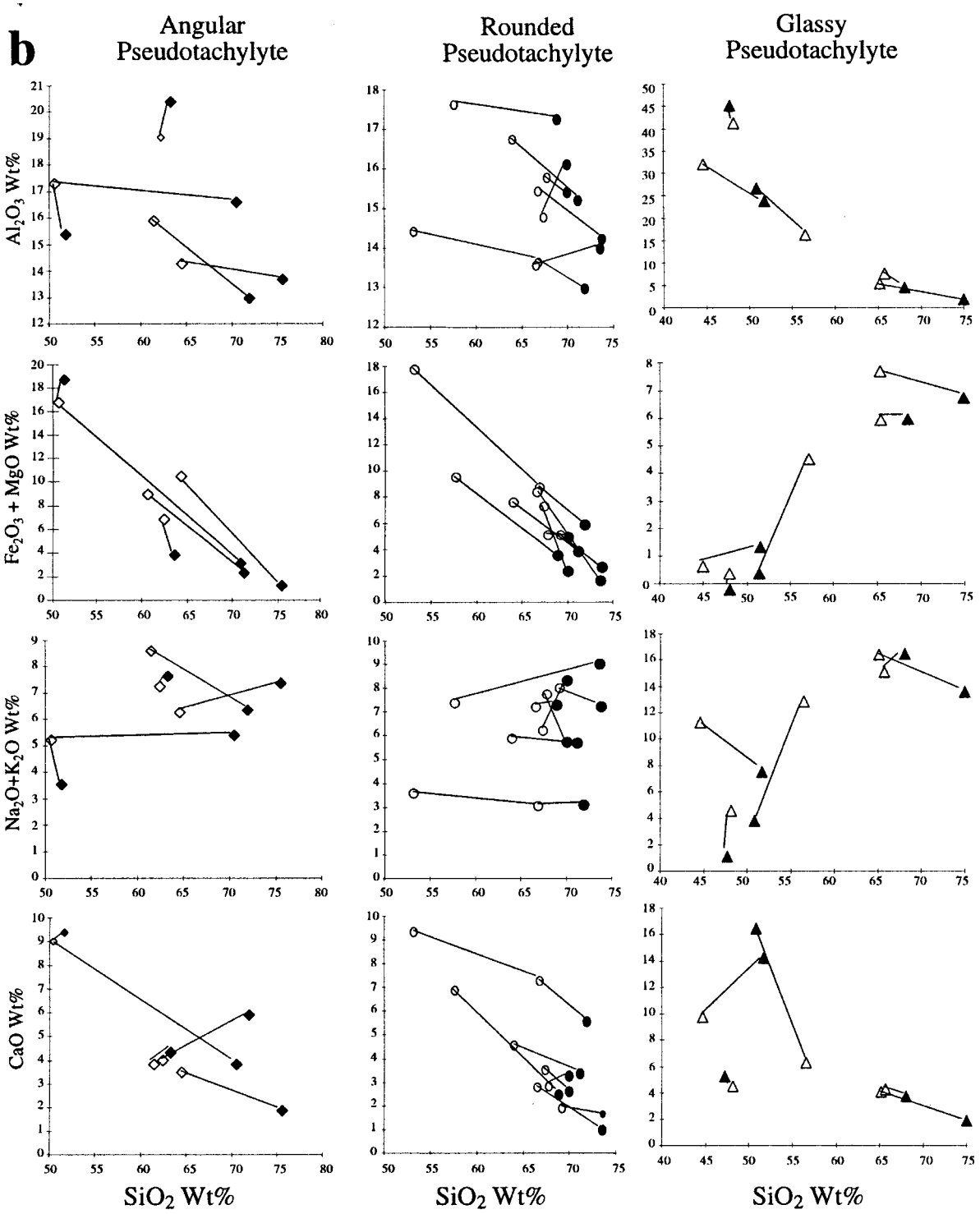

Fig. 6. (*continued*).

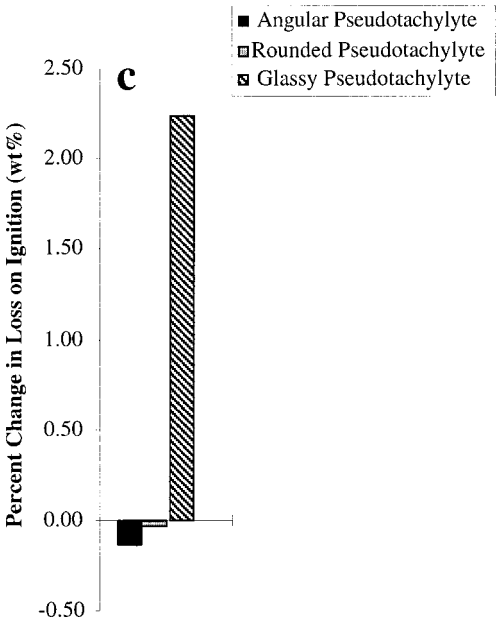

Fig. 6. (*continued*).

oxides seen in the DCP analysis. Point analyses made using the microprobe reveal a highly variable chemistry corresponding to individual quartz, feldspar, mica, and amphibole mineral compositions.

The textures, mineralogy, and chemistry of angular pseudotachylyte suggest that it formed by cataclasis, friction wear, and/or collapse of extensional microcrack walls during faulting. During this process the host rocks are ground to a fine powder, but individual mineral grains persist. Photomicrographs, SEM images, and microprobe analyses show that amphibole or mica grains are common in the fine-grained pseudotachylyte matrix, while most of the lithic clasts are rich in feldspar or quartz. Individual grains are distinct, surfaces are rough, and extinction patterns commonly show deformation twins and transgranular fractures, suggestive of cataclastic deformation. There is no textural evidence for solution transfer along grain boundaries, nor is there evidence for melting. These observations suggest that preferential crushing of hydrated mafic minerals (weaker phases) and exclusion of quartz and feldspar (stronger phases) account for the chemical changes (enrichment in metallic oxides, depletion in SiO_2 and Sr, and unchanging concentration of CaO and $A1_2O_3$) documented in angular pseudotachylyte.

5.2. Rounded pseudotachylyte

Rounded pseudotachylyte is found in reservoir zones, injection veins, and fault veins, and commonly exhibits flow textures (Fig. 7a). The pseudotachylyte consists of millimeter-scale lithic clasts in a microgranular matrix with sparse patches of isotropic material. Lithic clasts visible under optical microscope are commonly rounded, their centers have identifiable mineral grains, and their margins are commonly much finer grained and exhibit 120° triple junctions along neoblast boundaries. Clasts on all scales are rounded and interpenetrative forming a closely packed mass. Many clasts and grains exhibit well-developed haloes and recrystallized clast margins (Fig. 7b). SEM images show that the matrix is made up of interlocking grains that are either rounded or have polyhedral shapes (Fig. 7c and d). The same SEM images show large domains with conchoidal fracture and no visible crystal faces (Fig. 7e). These are interpreted as glassy domains within the mainly granular matrix.

XRD analyses of rounded pseudotachylyte show somewhat broad, depressed mineral peaks and higher levels of background noise than angular pseudotachylyte (Fig. 5b). This suggests that the pseudotachylyte matrix has a slightly lower degree of crystallinity than the host rock.

DCP chemical analyses of rounded pseudotachylyte show minor increases in the relative abundance of TiO_2, Fe_2O_3, and MgO relative to the host rock (Fig. 6a). Silica variation diagrams for rounded pseudotachylytes show significant increases in Fe_2O_3 and MgO compared to the host rocks; however, these increases are less steep than those observed in angular pseudotachylytes (Fig. 6b). Slight increases also occur in Al_2O_3, Sr and CaO. Minor decreases occur in the abundance of Na_2O and K_2O. Rounded pseudotachylytes show a minor decrease in loss on ignition relative to the host material (Fig. 6c). Microprobe analyses of rounded pseudotachylyte reveal a similar enrichment in metallic oxides, and show heterogeneous distribution of Al_2O_3, Na_2O, K_2O, and CaO. Haloes around the quartz- and feldspar-rich grains are particularly enriched in these elements in concert with the mineralogy of the surrounded clasts.

Rounded pseudotachylyte is interpreted as a sintered ultracataclasite, where sintering is defined as densification of a porous granular matrix by solution transfer mechanisms activated at high temperature (Luan and Patterson, 1992). Textures commonly include rounded to polyhedral, interlocking grains on microscopic scales. There are also rare patches of glassy material found in the rounded matrix. The compositional similarity between clasts and surrounding haloes suggests the operation of some form of solution-transfer, diffusion, or partial melting along grain boundaries (Magloughlin, 1992, 1998; Maddock, 1998). Similar textures and chemical relationships have been documented during experimental sintering or hot pressing of olivine (Schwenn and Goetze, 1978), calcite and quartz aggregates (Caristan et al., 1981), and natural

and synthetic quartz powders and gels (Luan and Patterson, 1992).

Sintering in granular material depends on chemistry, temperature, hydration, and grain size; the most commonly cited mechanisms are grain boundary diffusion, solution transfer, and partial fusion. All of these processes are active above the homologous temperature ($T_H = T/T_{Melting} > 0.6$–$0.7$) of the granular material (~700–900°C for granitic rocks). High water content, chemical impurities, and reduced grain size increase reaction rates. In experimental work carried out on natural silica/quartz powder (Luan and Patterson, 1992) extensive rounding and densification took place in less than 13 h at temperatures of 727–1027°C (Fig. 7f). Similar textures in rounded pseudotachylyte suggest that the initial ultracataclasite (angular pseudotachylyte) was heated to temperatures sufficient to cause extensive textural and chemical modification over a relatively short time-period (hours to days), but did not reach temperatures high enough (or of sufficient duration) for wholesale melting.

An alternative interpretation is that these textures represent melting confined to grain contacts in the pseudotachylyte matrix. Features that are commonly associated with grain surface melting include crystallites on porphyroclast margins, mineralogically complex transition zones between clasts and surrounding matrix, altered clast rims, and annealing of clast margins (Maddock, 1998; Magloughlin, 1998). Crystallites and complex transition zones are rare in the East Greenland pseudotachylyte suite; however, annealed and altered clast rims are more common (Fig. 7b and e), suggesting that these samples experienced elevated temperatures but not melting.

5.3. Glassy pseudotachylyte

Glassy pseudotachylyte is found most commonly in fault veins, with some isolated patches in injection

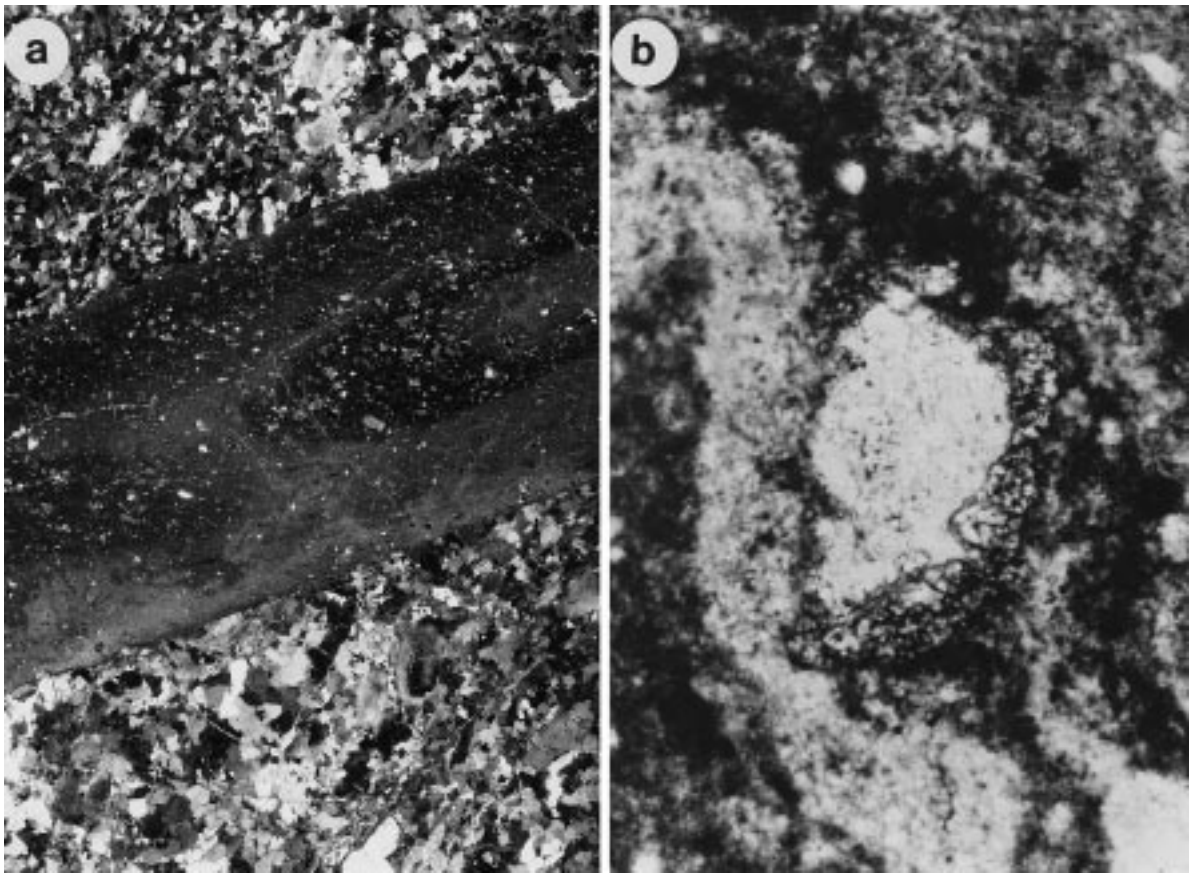

Fig. 7. Microstructures of rounded pseudotachylyte. (a) Injection vein with flow structures highlighted by shaded bands and aligned clasts. Sample 428449, 20 mm across, XPL. (b) Rounded clast with microcrystalline rim and undulose streamers of light colored material extending from the clast. Sample 428471, 0.5 mm across, XPL. (c) SEM image of rounded fragments, smooth indistinct clast surfaces, and a dense matrix of interlocking grains. Sample 428469, 200 μm across. (d) Detail of (c) showing indistinct grain edges and interlocking matrix, 20 μm across. (e) SEM image of rounded grains, polygonal grain/grain contacts, and interlocking grains. Sample 417427, 80 μm across. (f) SEM image of quartz powder sintered for 1 h at 1230°C (from Luan and Paterson, 1992), 100 μm across.

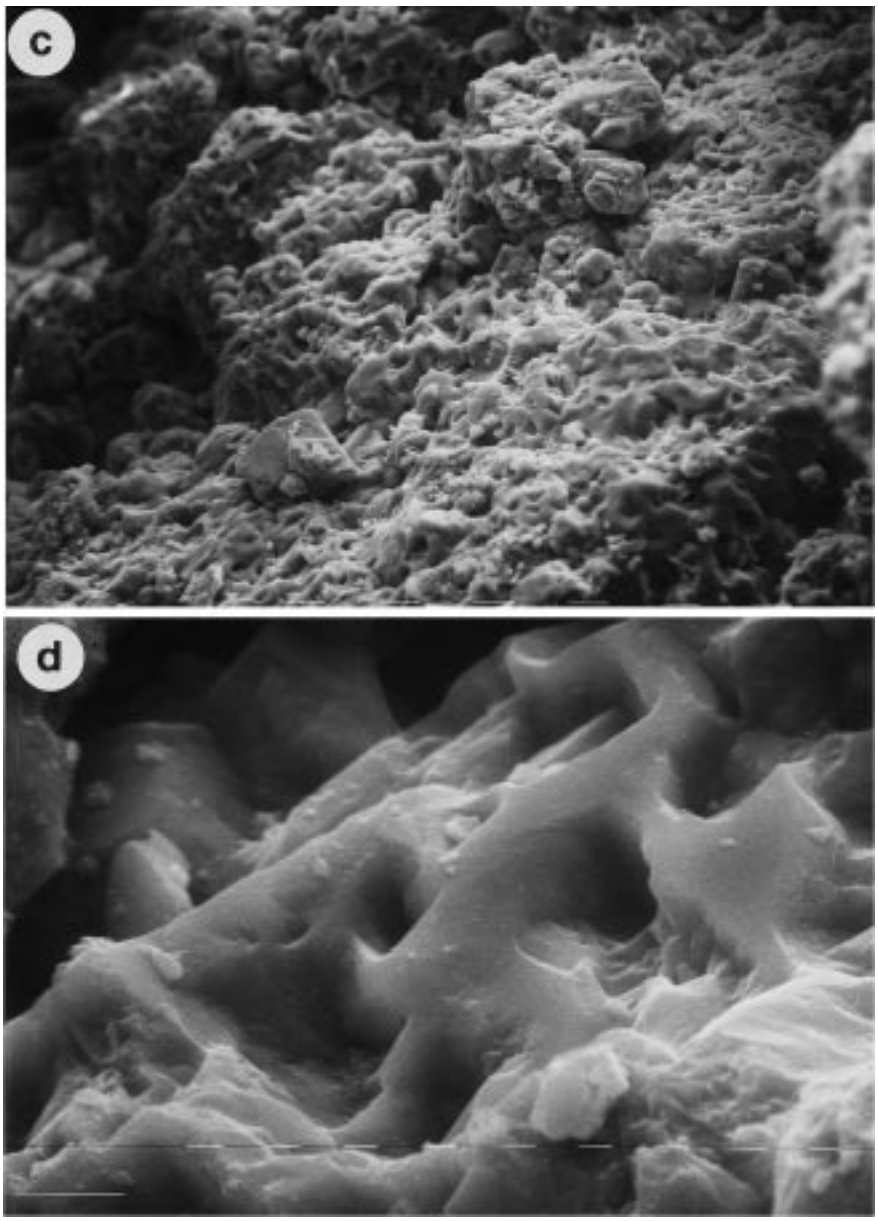

Fig. 7. (*continued*).

veins and minor amounts in reservoir zones. It consists of patches of optically isotropic pseudotachylyte that enclose strain-free, acicular, high-birefringence microlites in the isotropic matrix (Fig. 8a and b). Lithic clasts are uncommon, generally rounded, and have annealed, altered, or indistinct margins. SEM images show acicular crystal forms (Fig. 8c), rounded grains with strands of material bridging gaps between grains (Fig. 8d), and homogeneous, conchoidally fractured material interpreted as glass (Fig. 8d and e). There is a great resemblance between these glassy domains and SEM images of basaltic glass and obsidian (Fig. 8f).

XRD analyses of glassy pseudotachylyte show that there are significant differences between the mineralogy of the pseudotachylyte and the host rock (Fig. 5c), with the pseudotachylyte enriched in amphibole and mica relative to the host rock. Comparison between glassy pseudotachylyte XRD spectra and one of volcanic glass (Fig. 5d) show striking similarities, with high background to peak ratios and poorly defined mineral peaks indicating low-crystallinity amorphous material.

DCP chemical analyses indicate that the overall composition of many glassy pseudotachylyte samples is broadly andesitic, with less than 58% SiO_2, 14–17% Al_2O_3, and 10% $MgO + Fe_2O_3$ (Table 1). Glassy pseudotachylyte samples show increases in the abundance of TiO_2, Al_2O_3, Fe_2O_3, MgO, CaO, Na_2O, K_2O, Sr, and Ba relative to the host rock (Fig. 6a). Silica vari-

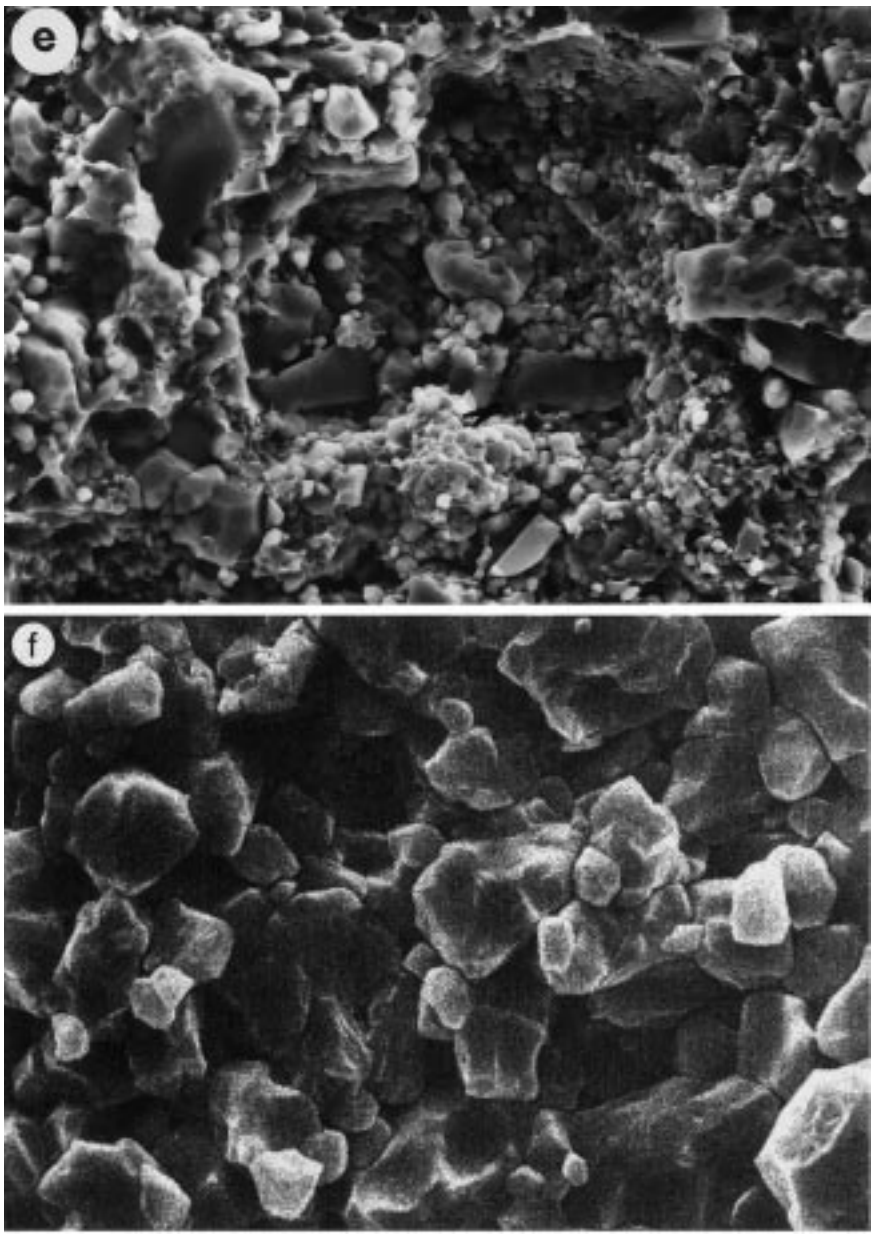

Fig. 7. (*continued*).

ation diagrams show mixed results: some samples show minor increases in some oxides relative to their host rocks, while other samples show significant decreases in those same oxides (Fig. 6b). Loss on ignition is higher in glassy pseudotachylyte than in its host rock, suggesting an increase in volatiles (Fig. 6c). Microprobe analyses of microlites indicate Fe-, Mg-rich amphiboles (cummingtonite or grunerite), in agreement with optical analysis. Microprobe analyses of the isotropic domains surrounding the amphibole microlites indicate that they have identical compositions.

The textural characteristics of glassy pseudotachylyte, its chemical composition, and its predominance in fault veins suggest that it forms as the result of frictional heating and melting of ultracataclasite during slip on fault planes. The andesitic composition of the glass, the amphibole mineralogy of the microlites, and the enrichment of the pseudotachylyte relative to the host rock in Fe_2O_3, MgO and TiO_2, reflect melting of hydrated mafic minerals that are preferentially included in the initial ultracataclasite (angular pseudotachylyte) as suggested by Spray (1992, 1995). The mineralogy of the microlites suggests that temperatures may have reached $>900^{\circ}C$, based on the melting tem-

perature of amphibole at low confining pressure (Deer et al., 1992).

6. Evolution of a pseudotachylyte-bearing fault zone

The following discussion addresses the formation of a pseudotachylyte-bearing fault zone in terms of the processes at work during seismic slip: initial faulting with accompanying cataclasis and grain size reduction, frictional heating, and finally melting (after Swanson, 1992). The distribution of the different pseudotachylyte types in distinct structural settings within East Greenland fault zones forms the basis for this discussion. Angular pseudotachylyte is found mostly in reservoir zones, suggesting that cataclastic textures are preserved in these areas and destroyed in other areas within the fault zone. Rounded pseudotachylyte is found in reservoir zones, injection veins, and fault veins, suggesting that frictional sliding generates enough heat to sinter or partially melt a significant fraction of the initial cataclasite. Glassy pseudotachylyte is generally confined to fault veins, suggesting that only along the primary slip surfaces is enough heat generated to melt the initial cataclastic material.

6.1. Fragmentation: formation of angular pseudotachylyte

Angular pseudotachylyte probably forms as a result of cataclasis during initial fracturing, fracture propagation, and frictional sliding. Fracture propagation and continued slip result in comminution and abrasive wear resulting from fracture linkage at the tips of faults (Swanson, 1992), spalling of the walls of extensional microfractures (Wenk, 1978; Weiss and Wenk, 1982), or asperity grinding during slip along the fault (Scholz, 1990). All of these processes contribute to the formation of ultracataclastic material (angular pseudotachylyte) by grain-size reduction in the fault zone. In East Greenland most of the angular pseudotachylyte is found in reservoir zones, and only minor amounts are

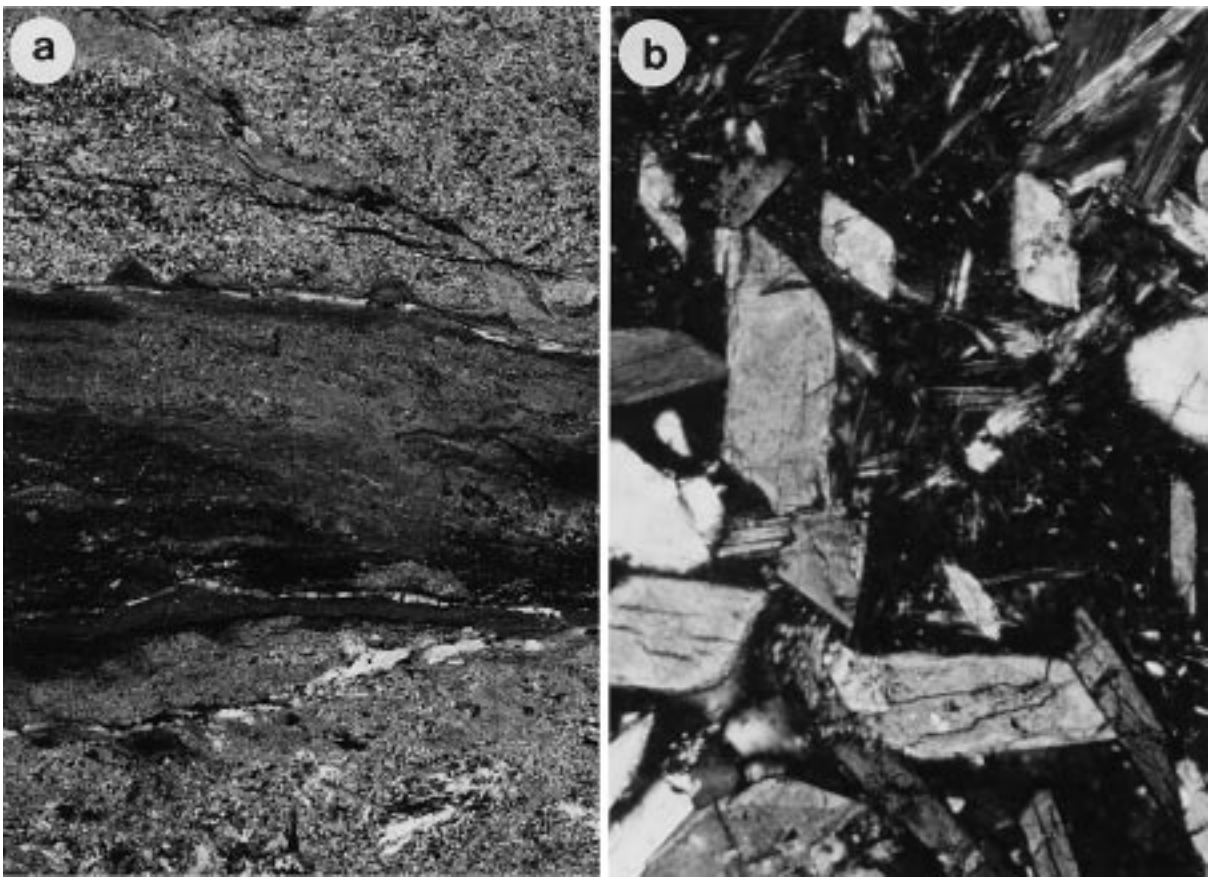

Fig. 8. Microstructures of glassy pseudotachylyte. (a) Fault vein containing isotropic patches, streaky color bands, and few clastic fragments. Sample 428472, 20 mm across, XPL. (b) Strain-free amphibole (cummingtonite) phenocrysts in isotropic matrix. Sample 438525, 0.5 mm across. (c) SEM image of acicular amphibole crystals. Sample 428472, 150 μm across. (d) SEM image of glassy fragment with conchoidal fracture in rounded matrix. Sample 428453, 50 μm across. (e) SEM image of conchoidally fractured material in crudely foliated matrix. Sample 91-234, 100 μm across. (f) SEM image of basaltic glass, 100 μm across.

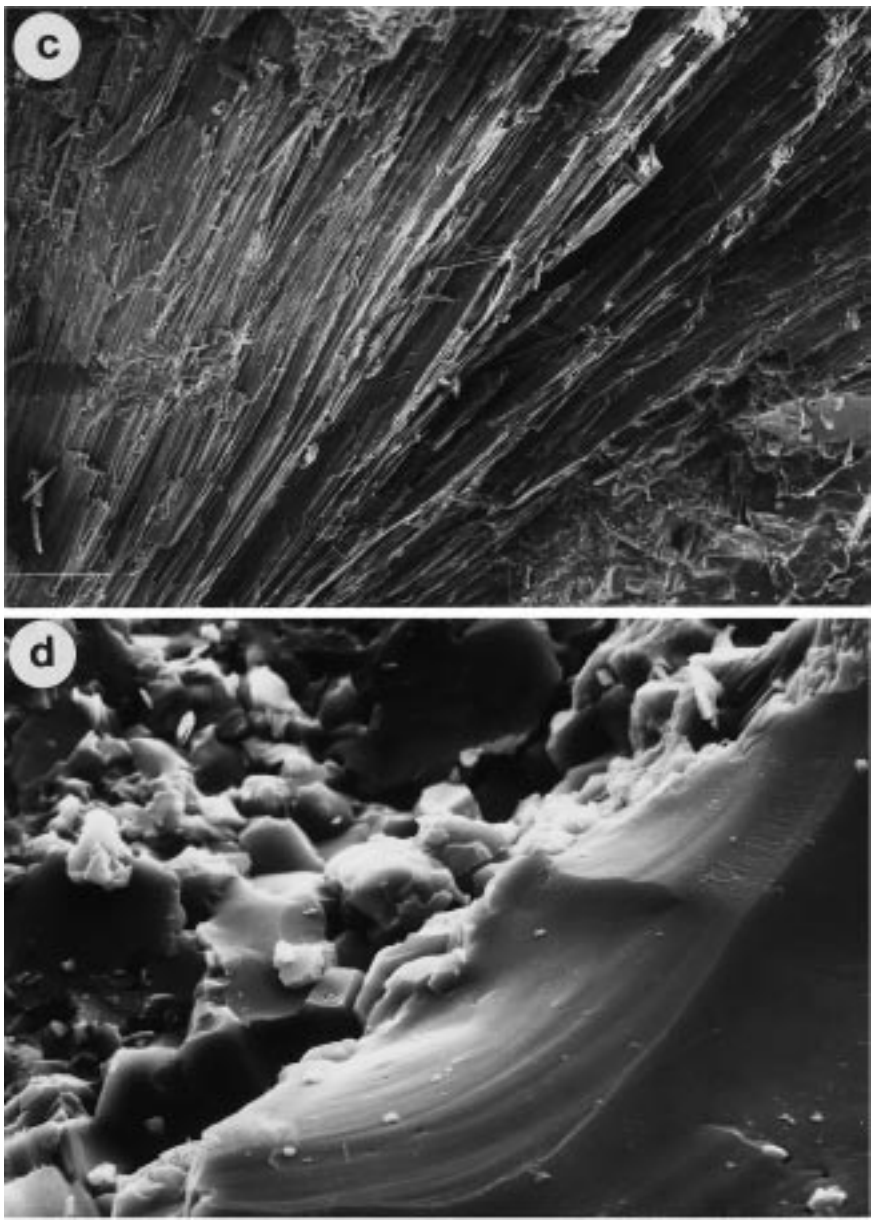

Fig. 8. (*continued*).

found in injection veins or fault veins. Therefore ultracataclastic textures of angular pseudotachylyte appear to be preferentially preserved in areas of little or no sustained frictional slip.

The enrichment in metallic oxides found in angular pseudotachylyte in East Greenland has also been documented in many other studies of pseudotachylyte, mainly in samples thought to have undergone melting (Dressler, 1984; Reimold, 1991; Magloughlin and Spray, 1992; Reimold and Colliston, 1994; Spray, 1995). This suggests that preferential crushing of mafic minerals during the formation of angular pseudotachylyte could heavily influence the compositions of rounded and glassy pseudotachylyte.

6.2. Frictional heating—sintering and formation of rounded pseudotachylyte

Once fracture propagation and frictional wear have produced ultracataclastic material (angular pseudotachylyte), the contact area on the fault surfaces is effectively increased (Swanson, 1992), as is the surface area to volume ratio in the cataclastic material. This comminuted material is then heated by continued (or later) frictional sliding. Material that escapes the fault surface into injection veins or reservoir zones will no longer be frictionally heated, and angular pseudotachylyte could be preserved in this way.

If the comminuted material undergoes some fric-

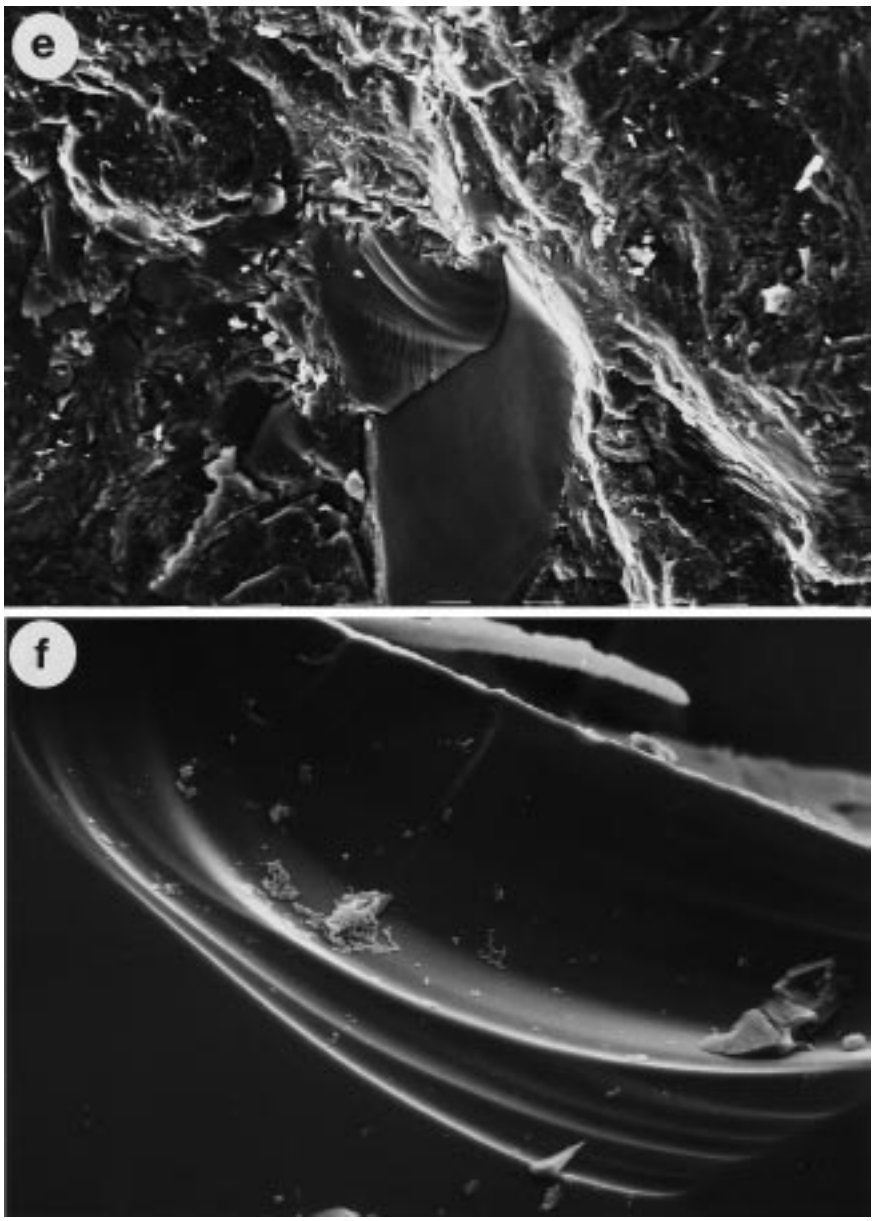

Fig. 8. (*continued*).

tional heating during slip and reaches the homologous temperature (T_H) of the constituent minerals, then sintering or hot pressing by grain-boundary diffusion or solution transfer (Schwenn and Goetze, 1978; Caristan et al., 1981) may occur. The textures and chemical relationships observed in rounded pseudotachylyte suggest that it formed by sintering, resulting in the characteristic grain shapes and densely packed, interlocking, polygonal grains. Temperatures above T_H (700–900°C) would only last for a few hours or days in a fault zone (McKenzie and Brune, 1972), so critical time/temperature relationships must have been satisfied in order to form the distinctive sintered textures. The presence of rounded pseudotachylyte in fault veins, injection veins and reservoir zones within pseudotachylyte-bearing faults indicates that frictional heating of ultracataclasite plays an important role in the formation of significant volumes of the East Greenland pseudotachylyte suite.

6.3. Melting—formation of glassy pseudotachylyte

Glassy pseudotachylyte is found mainly in fault veins and has, in its matrix, significant amounts of isotropic material and microlites. It exhibits conchoidal fractures at all scales, and has XRD spectra resembling that of natural glass. The chemical composition of the East Greenland pseudotachylyte glass is quite homo-

geneous, both within samples and among different samples, and is close to that of andesite. Crystals found in the isotropic glass are invariably Fe-, Mg-rich amphiboles (cummingtonite or grunerite) with crystallization temperatures around 900°C. The glass and the crystals have identical chemical compositions. These relationships suggest that glassy pseudotachylyte formed by melting of ultracataclasite during seismic slip.

6.4. Implications for tectonic environment

The large volumes of pseudotachylyte and the outcrop characteristics of many exposures found along fault zones in East Greenland are similar to pseudotachylyte outcrops found in meteorite impact structures. However, the East Greenland pseudotachylytes have an endogenic, tectonic origin related to continental rifting, and lack any of the distinctive features characteristic of hypervelocity impact sites (including shatter cones, ring structures, shocked mineral grains, preserved layers of ejecta).

Textural relationships, estimates of the temperatures reached during faulting (~700–900°C), and estimates of pseudotachylyte volume in individual outcrops broadly constrain the thermal energy imparted to the initial ultracataclasite. These estimates are used to derive rough values of seismic work and earthquake magnitude. Such estimates are fraught with assumptions about the actual volume of pseudotachylyte produced, the size and shape of the earthquake slip-patch, and the amount of pseudotachylyte produced during a single seismic event. Given the temperature constraints and the excellent exposure in East Greenland, however, these estimates provide rough maximum values of earthquake magnitude. The large volumes of pseudotachylyte in individual fault zones (some outcrops are >20 m on a side, i.e. Fig. 3d) and the relatively low temperatures (<700°C) indicated by preserved cataclastic textures in many samples suggest that the pseudotachylytes formed during relatively small earthquakes (moment magnitude (M_0) < 4). These estimates are in agreement with data from the Basin and Range (Sibson, 1982, 1983), indicating widespread, shallow microseismicity in a tectonic environment similar to the continental rift setting envisioned for the Tertiary in East Greenland. The widespread occurrence of pseudotachylyte in association with rift-related faults along nearly 400 km of the East Greenland margin indicates that microseismicity may have played an important role in accommodating deformation of the Tertiary East Greenland volcanic rifted margin.

7. Conclusions

Pseudotachylytes in fault veins, injection veins, and reservoir zones have been sampled from Early Tertiary normal faults and accommodation zones along nearly 400 km of the East Greenland volcanic rifted margin. Three textural types of pseudotachylyte have been identified: angular, rounded, and glassy. These textures vary between different structural settings, with angular pseudotachylyte found mainly in reservoir zones, rounded pseudotachylyte found in reservoir zones, injection veins and fault veins, and glassy pseudotachylyte found mainly in fault veins. Textural and chemical relationships in pseudotachylytes from these different mesoscopic settings suggest an evolutionary sequence of pseudotachylyte formation along fault zones. Initial frictional sliding and comminution produced ultracataclasite enriched in mica and amphibole fragments, with this texture preserved in reservoir zones. Heating and sintering of ultracataclasite occurred in fault veins, injection veins, and reservoir zones. Melting was generally confined to fault surfaces. The metal oxide enrichment observed in angular pseudotachylyte influences the chemistry of rounded and glassy pseudotachylyte. These observations, combined with independent information about paleo-crustal depths, lead to the interpretation that shallow, relatively small ($M_0 < 4$) earthquakes accompanied the rifting of East Greenland from Eurasia.

Acknowledgements

Thanks to J. G. Spray, M. T. Swanson, and T. Blenkinsop for their insightful and constructive reviews. Thanks to W. M. Meurer for assistance with DCP analyses, A. E. Boudreau for assistance with microprobe analyses, and L. Eibest for assistance with SEM analyses. This work is part of an ongoing comprehensive study of the Tertiary East Greenland volcanic rifted margin conducted by the Danish Lithosphere Center (DLC), which is funded by the Danish National Research Foundation. Structural studies were supported by the DLC and National Science Foundation grant EAR-9508250 (to Karson).

References

Bridgewater, D., Keto, L., McGregor, V.R., Myers, J.S., 1976. Archaean gneiss complex of Greenland. In: Escher, A., Watt, W.S. (Eds.), Geology of Greenland. The Geological Survey of Greenland, pp. 18–75.

Brooks, C.K., Nielsen, T.F.D., 1982. The Phanerozoic development of the Kangerdlugssuaq area, East Greenland. Meddelelser Øm Grønland Geoscience 9, 3–30.

Caristan, Y., Harpin, R.J., Evans, B., 1981. Deformation of porous

aggregates of calcite and quartz using the isostatic hot-pressing technique. Tectonophysics 78, 629–650.

Clift, P.D., Turner, J., ODP Leg 152 Scientific Party, 1995. Dynamic support by the Icelandic plume and vertical tectonics of the northeast Atlantic continental margins. Journal of Geophysical Research 100, 24473–24486.

Deer, W.A., Howie, R.A., Zussman, J., 1992. An Introduction to the Rock-forming Minerals. Longman Scientific & Technical, Essex.

Dressler, B.O., 1984. The effects of the Sudbury Event and the intrusion of the Sudbury Igneous Complex on the footwall rocks of the Sudbury Structure. In: Pye, E.G., Naldrett, A.J., Giblin, P.E. (Eds.), The Geology and Ore Deposits of the Sudbury Structure. Ontario Geological Survey Special Volume 1, pp. 97–138.

Eldholm, O., Grue, K., 1994. North Atlantic volcanic margins: dimensions and production rates. Journal of Geophysical Research 99, 2955–2968.

Erismann, T.H., 1979. Mechanisms of large landslides. Rock Mechanics 12, 15–46.

Gleadow, A.J.W., Brooks, C.K., 1979. Fission track dating, thermal histories, and tectonics of igneous intrusions in East Greenland. Contributions to Mineralogy and Petrology 71, 45–60.

Grocott, J., 1981. Fracture geometry of pseudotachylyte generation zones: a study of shear fractures formed during seismic events. Journal of Structural Geology 3, 169–178.

Hansen, K., 1996. Thermotectonic evidence of a rifted continental margin: fission track evidence from the Kangerlussuaq area, SE Greenland. Terra Nova 8, 458–469.

Karson, J.A., Brooks, C.K., 1999. Structural and magmatic segmentation of the Tertiary East Greenland volcanic rifted margin. In: Ryan, P., MacNiocall, C. (Eds.), Continental Tectonics. Geological Society, London, Special Publication, 164, 313–338.

Karson, J.A., Storey, M., Brooks, C.K., Pringle, M., 1998. Widespread Tertiary faulting and pseudotachylytes in the East Greenland Volcanic Rifted Margin: evidence of seismogenic faulting during magmatic construction. Geology 26, 39–42.

Kennedy, L.A., Spray, J.G., 1992. Frictional melting of sedimentary rock during high-speed diamond drilling: an analytical SEM and TEM investigation. Tectonophysics 204, 323–337.

Lambert, P., 1981. Breccia dikes: geological constraints on the formation of complex craters. In: Schultz, P.H., Merrill, R.B. (Eds.), Multi-ring Basins. Proceedings of the Lunar and Planetary Sciences 12A, pp. 59–78.

Larsen, H.C., Saunders, A.D., 1998. Tectonism and volcanism at the SE Greenland rifted margin: record of plume impact and later continental rupture. In: Saunders, A.D., Larsen, H.C., Wise, S. (Eds.), Proceedings of the Ocean Drilling Program, Scientific Results 152.

Larsen, H.C., 1990. The East Greenland Shelf. In: Grantz, A., Johnson, L., Sweeney, J.F. (Eds.), The Arctic Region, The Geology of North America L. Geological Society of America, pp. 185–210.

Larsen, H.C., Saunders, A.D., Clift, P. et al., 1994. Proceedings of the Ocean Drilling Program, Initial Reports 153. Ocean Drilling Program, College Station, Texas.

Luan, F.C., Patterson, M.S., 1992. Preparation and deformation of synthetic aggregates of quartz. Journal of Geophysical Research 97, 301–320.

Maddock, R.H., 1998. Pseudotachylyte formed by frictional fusion. In: Snoke, A.W., Tullis, J., Todd, V.R. (Eds.), Fault-related Rocks: A Photographic Atlas. Princeton University Press, Princeton, NJ, pp. 80–87.

Magloughlin, J.F., Spray, J.G., 1992. Frictional melting processes and products in geological materials: introduction and discussion. Tectonophysics 204, 197–206.

Magloughlin, J.F., 1998. Melting relations within lithic clasts in pseudotachylyte. In: Snoke, A.W., Tullis, J., Todd, V.R. (Eds.), Fault-related Rocks: A Photographic Atlas. Princeton University Press, Princeton, NJ, pp. 90–91.

Magloughlin, J.F., 1992. Microstructural and chemical changes associated with cataclasis and frictional melting at shallow crustal levels: the cataclasite–pseudotachylyte connection. Tectonophysics 204, 243–260.

Masch, L., Wenk, H.R., Preuss, E., 1985. Electron microscopy study of hyalomylonites—evidence for frictional melting in landslides. Tectonophysics 115, 131–160.

McKenzie, D., Brune, J.N., 1972. Melting on fault planes during large earthquakes. Geophysical Journal of the Royal Astronomical Society 29, 65–78.

Mosher, S., 1976. Pressure solution as a deformation mechanism in Pennsylvanian conglomerates from Rhode Island. Journal of Geology 84, 355–364.

Myers, J.S., 1980. Structure of the coastal dyke swarm and associated plutonic intrusions of East Greenland. Earth and Planetary Science Letters 46, 407–418.

Nielsen, T.F., Brooks, C.K., 1981. The East Greenland rifted continental margin: an examination of the coastal flexure. Journal of the Geological Society of London 138, 559–568.

Nielsen, T.F.D., 1975. Possible mechanism of continental breakup in the North Atlantic. Nature 253, 182–184.

Nielsen, T.F.D., 1978. The Tertiary dike swarms of the Kangerdlugssuaq area, East Greenland: an example of magmatic development during continental breakup. Contributions to Mineralogy and Petrology 67, 63–78.

Pedersen, A.K., Watt, M., Watt, W.S., Larsen, L.M., 1997. Structure and stratigraphy of the Early Tertiary basalts of the Blosseville Kyst, East Greenland. Journal of the Geological Society of London 154, 565–570.

Reimold, W.U., Colliston, W.P., 1994. Pseudotachylites of the Vredefort Dome and the surrounding Witwatersrand Basin, South Africa. In: Dressler, B.O., Grieve, R.A.F., Sharpton, V.L. (Eds.), Large Meteorite Impacts and Planetary Evolution. Geological Society of America Special Paper 293, pp. 177–196.

Reimold, W.U., 1991. The geochemistry of pseudotachylytes from the Vredefort Dome, South Africa. Neues Jahrbuch fürMineralogische Abhandlung 162, 151–184.

Scholz, C.H., 1990. The Mechanics of Earthquakes and Faulting. Cambridge University Press, New York.

Schwenn, M.B., Goetze, C., 1978. Creep of olivine during hot-pressing. Tectonophysics 48, 41–60.

Scott, J.S., Drever, H.I., 1953. Frictional fusion along a Himalayan thrust. Proceedings of the Royal Society of Edinburgh 65, 121–142.

Shimamoto, T., Nagahama, H., 1992. An argument against the crush origin of pseudotachylytes based on the analysis of clast-size distribution. Journal of Structural Geology 14, 999–1006.

Sibson, R.H., 1975. Generation of pseudotachylyte by ancient seismic faulting. Geophysical Journal of the Royal Astronomical Society 43, 775–794.

Sibson, R.H., 1982. Fault zone models, heat flow, and the depth distribution of earthquakes in the continental crust of the United States. Bulletin of the Seismological Society of America 72, 151–163.

Sibson, R.H., 1983. Continental fault structure and the shallow earthquake source. Journal of the Geological Society of London 140, 741–767.

Spray, J.G., Thompson, L.M., 1995. Friction melt distribution in a multi-ring impact basin. Nature 373, 130–132.

Spray, J.G., 1987. Artificial generation of pseudotachylyte using friction welding apparatus: simulation of melting on a fault plane. Journal of Structural Geology 9, 49–60.

Spray, J.G., 1989. Slickenside formation by surface melting during the mechanical excavation of rock. Journal of Structural Geology 11, 895–905.

Spray, J.G., 1992. A physical basis for the frictional melting of some rock forming minerals. Tectonophysics 204, 205–221.

Spray, J.G., 1995. Pseudotachylyte controversy: fact or friction? Geology 23, 1119–1122.

Spray, J.G., 1997. Superfaults. Geology 25, 579–582.

Swanson, M.T., 1992. Fault structure, wear mechanisms and rupture processes in pseudotachylyte generation. Tectonophysics 204, 223–242.

Tegner, C., Duncan, R.A., Bernstein, S., Brooks, C.K., Bird, D.K., Storey, M., 1998. ^{40}Ar–^{39}Ar geochronology of Tertiary mafic intrusions along the East Greenland rifted margin: relation to flood basalts and the Iceland hotspot track. Earth and Planetary Science Letters 156, 75–88.

Thompson, L.M., Spray, J.G., 1994. Pseudotachylytic rock distribution and genesis within the Sudbury impact structure. In: Dressler, B.O., Grieve, R.A.F., Sharpton, V.L. (Eds.), Large Meteorite Impacts and Planetary Evolution. Geological Society of America Special Paper 293, pp. 27–87.

Wager, L.R., Deer, W.A., 1938. A dyke swarm and crustal flexure in East Greenland. Geological Magazine 75, 39–46.

Weiss, L.E., Wenk, H.R., 1982. Al-rich calcic pyroxene in pseudotachylyte: An indicator of high pressure and high temperature? Tectonophysics 84, 329–341.

Wenk, H.R., 1978. Are pseudotachylyte products of fracture or fusion? Geology 6, 507–511.